Single-Crystal ^{27}Al NMR of Andalusite and Calculated Electric Field Gradients: the First Complete NMR Assignment for a 5-Coordinate Aluminum Site

Pamela L. Bryant, Chris R. Harwell, Katherine Wu, Frank R. Fronczek, Randall W. Hall,* and Leslie G. Butler*

Department of Chemistry, Louisiana State University, Baton Rouge, Louisiana 70803

Received: February 1, 1999; In Final Form: April 19, 1999

Andalusite, Al_2SiO_5, contains 5- and 6-coordinate aluminum sites, and is a preeminent model for ^{27}Al NMR spectroscopy. We describe a combined NMR, crystallography, and theory project: single-crystal ^{27}Al NMR spectra at 298 K, the crystal structure of andalusite at 115 K, and electric field gradient calculations. The low-symmetry 5-coordinate site is a stiff test of the computational methods. In addition, the chemical shift tensor is measured for the 5-coordinate site. The small body of ^{27}Al NMR data, especially for rare 5-coordinate sites, inspires the calculation of NMR parameters. We explore the accuracy of two approaches for ^{27}Al EFG calculations: first, ab initio molecular orbital calculations of small clusters embedded in an array of point charges; second, full-potential linearized augmented plane wave density functional calculations of the crystal. The agreement between the experimental EFG orientation and that from the full-crystal density functional theory is remarkably close, differing by only 0.17° for the 6-coordinate site and 1.56° for the 5-coordinate site. The calculated value of C_q is in error by −0.254 MHz for the 5-coordinate site. The embedded cluster molecular orbital results are significantly less accurate, with orientation errors exceeding 45°.

Introduction

Andalusite, kyanite, and sillimanite all share the Al_2SiO_5 formula, yet only andalusite has a 5-coordinate aluminum site.[1] All three minerals have been extensively studied via NMR and NQR, including single-crystal NMR, yet of the eight aluminum sites in these three minerals, five sites remain unassigned.[2−11] Ambiguities exist in the assignment of the 5-coordinate site in andalusite and all four octahedral sites in sillimanite. The three assignments were made using symmetry arguments.[2,3] Point charge models proved insufficient to assign the remaining five sites.[5]

The failure to assign well-measured ^{27}Al NMR spectra to specific aluminum sites is due to a lack of interpretative tools. This impedes progress in important areas of research. For example, ^{27}Al NMR spectroscopy of methylaluminoxane (MAO)[12−17] has, to date, relied only on chemical shifts, and structure elucidation is not complete.[18−21] The inclusion of quadrupolar information is seen as another structural tool. Recently, 5-coordinate[22] and 6-coordinate[23] sites in powder samples have been characterized by both chemical shift and quadrupolar interactions.

The connection between structure and ^{27}Al quadrupolar interaction has been made with point charge models[5] and shear strain correlations;[24,25] the latter are correlations between the ^{27}Al quadrupole coupling constant and distortion of a tetrahedral or octahedral environment at an aluminum site. In the aluminophosphates, shear strain correlations were used to reassign the VPI-5 (hydrated) ^{27}Al NMR spectrum[26] and to partially assign $AlPO_4$−18, (hydrated)[27] but were insufficient to completely assign the spectrum for the calcined or methanol saturated $AlPO_4$−18[27] or sites in $AlPO_4$−5 or $AlPO_4$−11.[28]

The procedure used herein pertains to static systems. Andalusite has a rigid lattice. The phase diagram for the Al_2SiO_5 system shows andalusite as the stable phase at 300 K, 1 atm, with kyanite the stable high pressure phase, and possibly more stable at low temperature.[29,30] The andalusite structure was determined at 115 K and there is no evidence of a phase change in the temperature range of 20 [31] to 1273 K.[32]

The 5-coordinate site in andalusite is approximately trigonal bipyramidal, a coordination geometry found in other minerals[33−37] aluminates,[38,39] aluminum alkyloxides[40−42] organometallic clusters,[43,44] and aluminophosphates such as $AlPO_4$−21.[45] Square pyramidal aluminum coordination has also been observed in a Salen complex[46] and in sodium aluminoglycolate.[47]

Fully assigned ^{27}Al electric field gradient tensors are rare. Gas-phase microwave spectroscopy, very successful for ^{2}H, ^{14}N, and ^{17}O, has been employed once for a polyatomic aluminum species, $(CH_3)_3NAlH_3$.[48] Single-crystal ^{27}Al NMR results are available for a number of minerals, yet the assignments are generally complete only for the high-symmetry sites, i.e., an asymmetry parameter near zero. Previous to this work, there were no 5-coordinate aluminum sites for which the EFG or CSA tensor orientations were known. EFG tensor orientations are needed to further develop interpretative models for ^{27}Al NMR spectroscopy.

Embedded cluster molecular orbital[49−53] (MO) and full-crystal density functional theory[54−60] (DFT) methods have been used previously to calculate EFG tensors of solids. The most accurate embedded cluster MO calculations have used a small, charged cluster embedded in a lattice of point charges. Despite the relatively small cluster size, this approach has been shown to give good results for sites with some symmetry (such as axial symmetry): CaF_2 [52] and spinels.[50] It is useful to investigate the limits of an embedded cluster MO method because it can be used to study disordered systems, as opposed to full-crystal DFT approaches. Full-crystal DFT studies have been successful in studying periodic systems and, hence, provide a benchmark for the embedded cluster MO methods, as well as allowing study

* To whom correspondence should be addressed.

10.1021/jp990374i CCC: $18.00
Published on Web 06/17/1999

of highly asymmetric sites. These two methods have been applied to a variety of Al-containing systems. Corundum, α-Al_2O_3, has been a test of calculations for systems with an infinite covalent network[61−67] and the subject of the first complete measurement of the ^{27}Al chemical shift anisotropy.[68] Small clusters have been studied as models for aluminosilicates and zeolites.[69−72] In related work, the ^{25}Mg and ^{17}O EFGs in the mineral forsterite, Mg_2SiO, were calculated with impressive accuracy with DFT methods.[58]

The comparison of calculated to experimental EFG tensors should be done with an awareness of the site symmetry. In very high-symmetry sites, the orientation of the EFG tensor is known a priori, thus, the only independent parameter is the quadrupole coupling constant, $C_q = e^2q_{zz}Q/h$. The 5-coordinate site in andalusite has *m*-point symmetry, permitting three independent parameters in the EFG tensor: the quadrupole coupling constant, asymmetry parameter, and one angle specifying the orientation of the EFG tensor with respect to the crystal axis system. In this work, we combine single-crystal ^{27}Al NMR with calculations to generate the first complete assignment of the ^{27}Al NMR parameters, both electric field gradient and chemical shift tensors, for a 5-coordinate aluminum site.

Experimental Section

NMR Spectroscopy. A single-crystal of pinkish-yellow andalusite was cut into a rough rectangular prism (3 mm × 3.6 mm × 4.7 mm) and the remainder crushed into a powder in a stainless steel mill. Small crystals from the powder were examined by single-crystal X-ray diffraction at 293 and 115 K (vida infra); the former is identical to a recent 295 ± 2 K report.[73]

Single-crystal NMR spectra were collected on a Chemagnetics Infinity 400 MHz spectrometer at 298 K with a novel single-crystal NMR probe; an optical encoder, mounted on the sample rotation shaft, is used to measure the rotation angle. Spectra were acquired over a frequency range of 101.7−106.8 MHz (0 ppm = 104.244187 MHz; magnet drift about 5 Hz (^{27}Al signal) over the 4 days). The pulse sequence was a single 1 μs pulse (90° = 4.75 μs for 1 M $Al(NO_3)_3$) with a relaxation delay of 0.2 s. Typically, 200 to 1000 scans were recorded per orientation. The crystal was rotated about three crystallographic axes with an increment of 3° over a 235° range. The $|+1/2\rangle \rightarrow |-1/2\rangle$ transition line widths were about 5 kHz (fwhh); the satellite transitions were 10 kHz. The orientation of the crystal in the plexiglass cube holder[74] was checked with single-crystal X-ray diffraction on an Enraf−Nonius CAD4 diffractometer, and the orientation matrix was used in the data analysis. In the data analysis, small errors, 6.19°, 4.97°, and −0.26° for *a*, *b*, and *c* rotations, respectively,[75] in the crystal holder orientation (cube holder did not lay flat in the rotating shaft) were noted and corrections made on the basis of the rotation pattern of the 6-coordinate site with 2-site symmetry. The data analysis was done with a least-squares fit to all symmetry-related data for $|+1/2\rangle \rightarrow |-1/2\rangle$, $|+3/2\rangle \rightarrow |+1/2\rangle$, and $|-1/2\rangle \rightarrow |-3/2\rangle$ transitions with independent parameters as elements of the EFG and chemical shift tensors. In the refinement, initial values of the EFG tensor were obtained with the Volkoff method.[76,77] The isotropic chemical shifts were constrained to be 10 and 35 ppm for the 6- and 5-coordinate sites, respectively.[7] The single-crystal data and fits for the 5-coordinate site are shown in Figures 1 and 2, the EFG tensors are given in Table 1, and the chemical shift tensors in Table 2.

X-Ray Crystallography. Diffraction data were collected on an Enraf−Nonius CAD4 diffractometer equipped with MoKα radiation and a graphite monochromator. The sample temperature was maintained by an Enraf−Nonius N_2 gas stream cryostat. Accurate unit cell parameters were obtained by least-squares refinement vs sin θ/λ values for 25 reflections (12° < θ < 17°). Data reduction included corrections for background, Lorentz, and polarization effects and absorption corrections based on ψ scans. Standard reflections indicated no intensity decay during data collection. Beginning coordinates were those of Burnham and Buerger.[78] Refinement was by full-matrix least-squares, with neutral atom scattering factors and anomalous dispersion corrections. All atoms were refined anisotropically. Calculations were carried out using the MolEN programs.[79] Refinement data is listed in Table 3. Atomic positions are listed in Table 4, and bond distances are given in Table 5. Cell dimensions for the same crystal at 293 K were a = 7.7932(4),

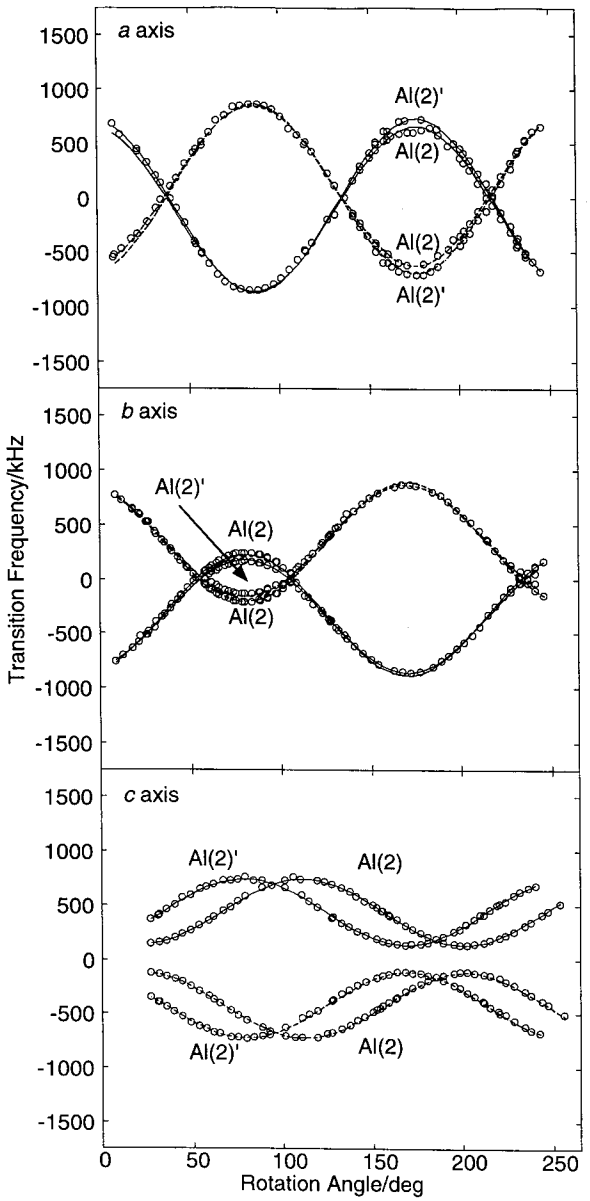

Figure 1. Single-crystal ^{27}Al NMR transition frequencies (○) for the two magnetically inequivalent 5-coordinate sites in andalusite, Al(2) and Al(2)′. Relative to the fractional coordinates given in Table 4, Al-(2) is at (x, y, 1/2) and (1 − x, 1 − y, 1/2) and Al(2)′ is at (1/2 − x, 1/2 + y, 0), and (1/2 + x, 1/2 − y, 0). The least-squares fit to the $|+3/2\rangle \rightarrow |+1/2\rangle$ transition is shown as a solid line; the $|-1/2\rangle \rightarrow |-3/2\rangle$ transition is shown as a dashed line. The sign of the quadrupole coupling constant is taken from the full-crystal DFT calculations (Table 1).

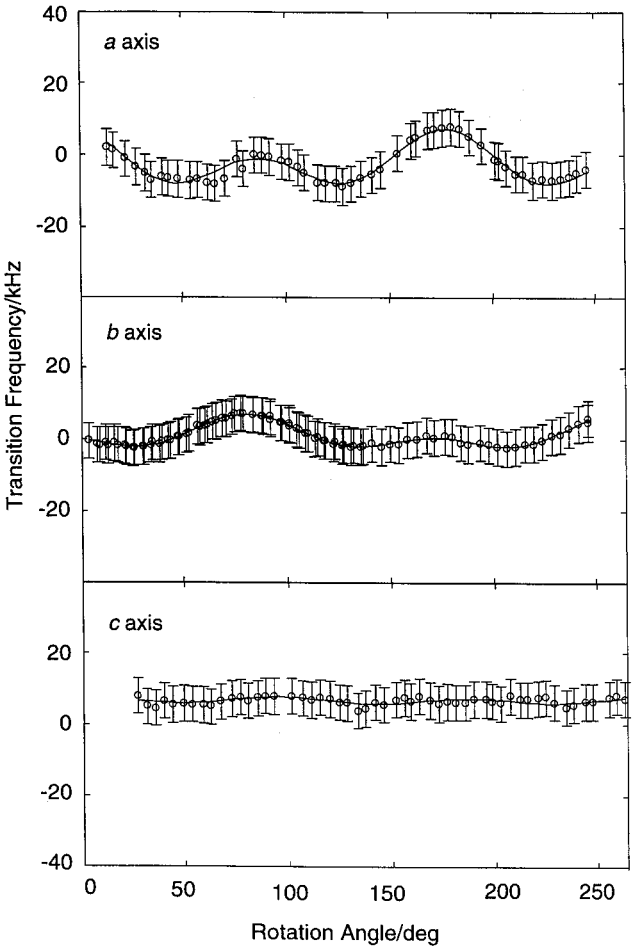

Figure 2. The least-squares fit to the $|+1/2\rangle \rightarrow |-1/2\rangle$ transition for both Al(2) and Al(2)′. The error bars are drawn at ±1/2 fwhh for the measured transition frequencies.

$b = 7.8978(3)$, $c = 5.5538(2)$Å, $V = 341.83(4)$ Å^3. Preliminary results from a 20 K single-crystal experiment of the same sample showed no change in structure.[31]

Calculations. *Embedded Cluster Molecular Orbital Calculations.* The crystal lattice was simulated by a neutral system of 864 sites or 27 unit cells ($3 \times 3 \times 3$) to minimize edge effects. Each site was occupied by a point charge, except for a center region consisting of a small, negatively charged AlO_x cluster. The 6-coordinate site, AlO_6^{-9}, was embedded in a lattice of 857 point charges; 858 point charges were used for the 5-coordinate site, AlO_5^{-7}. The point charges were given their oxidation numbers as point charges, −2, +3, and +4 for O, Al, and Si sites, respectively, and placed at locations corresponding to the 115 K andalusite structure. No attempt was made to self-consistently determine the optimum values for the point charges using the molecular orbital calculations. The calculations were performed with *Gaussian92*/DFT, Revision F.4[80] at the Hartree−Fock level using a variety of basis sets (see Table 6). Some additional calculations were performed at the MP2 and CI level, without any qualitative differences. We investigated the effect of both polarization and diffuse functions as both types of functions have been used in the past to study ionic and partially ionic crystals.[81−85]

Full-Crystal Density Functional Calculations. WIEN97[86] was used to perform full-potential linearized augmented plane wave (FP-LAPW) calculations on the andalusite crystal. Coordinates were taken from the 115 K structure. The generalized gradient approximation (GGA) for the exchange correlation potential, V_{xc}, was used.[87−89] The Kohn−Sham equations were solved by linear variation of LAPW. A linear combination of the product of radial functions and spherical harmonics was used inside the atomic spheres, while between them, in the interstitial region, a plane wave expansion was used. The convergence cutoff, $R_{mt}\,K_{max}$, for this LAPW expansion ranged from 3 to 6.76. R_{mt}, the smallest atomic sphere radius, was 1.2 au; K_{max}, the magnitude of the largest K vector, was 5.63333 a_o^{-1}. The irreducible wedge of the Brillouin zone was sampled with up to 128 k-points. The k-mesh was shifted away from high-symmetry directions. G_{max}, the magnitude of largest vector in the charge density Fourier expansion, was 24 a_o^{-1}. A total of 10 000 plane waves were used. No shape approximations were made for the potential or the electronic charge density. Inside the atomic spheres, spherical harmonics up to $l = 6$ were used. These values are comparable to those used in a previous study of forsterite.[58] Total energy was shown to be self-consistent to 0.0001 Ryd for three consecutive iterations. Additional calculations with up to 512 k-points showed no qualitative differences.

The nuclear electric quadrupole moment used for ^{27}Al is $140.3(1.0) \times 10^{-31}$ m^2, and the conversion factors for both the embedded cluster MO and full-crystal DFT calculations are given in the references.[90,91]

Results

The ^{27}Al NMR resonances for the four magnetically inequivalent aluminum sites in andalusite are assigned by a combination of three key projects: room-temperature single-crystal ^{27}Al NMR spectroscopy, 115 K X-ray structure determination, and the calculation of EFG tensors with embedded cluster MO and DFT theories. This work yields the unambiguous assignments of the EFG tensor orientations for the four magnetically inequivalent aluminum sites in andalusite and the sign of the quadrupole coupling constant for both aluminum coordinations. In addition, the chemical shift tensor is determined for the 5-coordinate site. This is the first full assignment of a 5-coordinate site in solid-state ^{27}Al NMR spectroscopy.

The single-crystal NMR results, Figures 1 and 2 and Table 1, found here at 298 K are in good agreement with those found earlier with room temperature single-crystal ^{27}Al NMR[3] and with 77 K NQR[6] (see Table 7).

The orientation of the EFG principal axis for the 6-coordinate site is nearly collinear with the Al(1)−O(4) bond, to within 2.0°, the same orientation found by Hafner, et al.[3] The orientation of the EFG tensor for the 5-coordinate site is shown in Figure 3. The 5-coordinate site can be described as a trigonal bipyramid with O(1) and an O(3) in axial sites. The EFG tensor lies approximately aligned with the trigonal bipyramid: the EFG *y*-axis is roughly aligned with the major axis of the trigonal bipyramid, and the EFG *x*-axis is nearly aligned with one of the equatorial oxygens, an O(3); $\angle eq_{zz}$,(Al(2)−O(3)) = 6.3°. As required by site symmetry, one EFG component is aligned with the crystal *c*-axis; $eq_{zz} \parallel c$. It is interesting that eq_{zz} lies in the equatorial plane rather than aligned along the axis of the trigonal pyramid.

The ^{27}Al chemical shift tensor for the 5-coordinate site is given in Table 2. Also listed, for completeness, are the results for the 6-coordinate site; however, these are much less precise. The large errors for the 6- relative to the 5-coordinate site illustrate the difficulty of measuring a small chemical shift interaction in the presence of a large quadrupolar interaction. This problem has recently been discussed in a single-crystal ^{2}H NMR project.[92] The chemical shift anisotropy, $\Delta\delta = \delta_{33} - (1/2)\,(\delta_{11} + \delta_{22})$,[93] is not expected to be large for an aluminum-

TABLE 1: Measured and Calculated EFG Tensors (in MHz) in the Crystal Axis System[a]

source	6-coordinate site, Al(1)[b]			∠eq_{zz}, *a*-axis	∠eq_{yy}, *c*-axis	5-coordinate site, Al(2)[c]			∠eq_{zz}, *c*-axis	∠eq_{yy}, *b*-axis
NMR	10.229(3)[d]	9.269(4)	0	28.50°[f]	0°	−1.2462(5)[e]	−1.0328(5)	0	0°	15.87°
(this work)	9.269(4)	−1.814(3)	0			−1.0328(5)	−4.5861(6)	0		
	0	0	−8.416(4)			9	9	5.8323(8)		
NMR [3]	10.46	9.83	0	34.09°	0°	−1.202	−1.144	0	0°	16.60°
	9.83	−2.59	0			−1.144	−4.698	0		
	0	0	−8.42			0	0	5.900		
FC-DFT[g]	9.076	8.344	0	28.67°	0°	−0.920	−1.020	0	0°	14.31°
	8.344	−1.617	0			−1.020	−4.658	0		
	0	0	−7.459			0	0	5.578		
EC-MO[h]	10.615	10.008	1.924	27.73°	59.47°	−2.549	−1.308	−2.630	18.50°	59.51°
	10.008	−3.283	−0.093			−1.308	−1.912	−0.387		
	1.924	−0.093	−7.332			−2.630	−0.387	4.461		

[a] EFG tensors given in the crystal axis system: $x \| a$, $y \| b$, $z \| c$. [b] Sites (0, 0, z) and (0, 0, 1 − z). For sites (1/2, 1/2, 1/2 − z) and (1/2, 1/2, 1/2 + z), the signs of the *ab* and *ba* elements are negative. [c] Sites (x, y, 1/2) and (1 − x, 1 − y, 1/2). For sites (1/2 − x, 1/2 + y, 0) and (1/2 + x, 1/2 − y, 0), the signs of the *ab* and *ba* elements are positive. [d] Error limits are given as 1σ. [e] Error limits are given as 1σ. [f] Components of the EFG tensors (eq_{xx}, eq_{yy}, eq_{zz}) are given in their principal axis system. [g] Table 6: Full Crystal Density Functional Theory, $R_{mt} \times K_{max} = 6.76$. [h] Table 6: Embedded Cluster Molecular Orbital Theory, 6-31G(3df).

TABLE 2: Chemical Shift Tensors (in ppm) in the Crystal Axis System[a]

6-coordinate site, Al(1)[b]			5-coordinate site, Al(2)[c]		
28(46)	−4(54)	0	25(13)	17(16)	0
−4(54)	33(44)	0	17(16)	76(14)	0
0	0	−32(63)	0	0	5(16)

[a] Chemical shift tensors given in the axis system: $x \| a$, $y \| b$, $z \| c$. [b] Sites (0, 0, z) and (0, 0, 1 − z). For sites (1/2, 1/2, 1/2 − z) and (1/2, 1/2, 1/2 + z), the signs of the *ab* and *ba* elements are positive. [c] Sites (x, y, 1/2) and (1 − x, 1 − y, 1/2). For sites (1/2 − x, 1/2 + y, 0) and (1/2 + x, 1/2 − y, 0), the signs of the *ab* and *ba* elements are negative.

TABLE 3: Crystal, Experimental, and Refinement Data for Andalusite at 115 K

mol formula	$SiAl_2O_5$
fw	165.05
cryst syst	orthorhombic
space group	*Pnnm*
temp	115 K
cell constants	
a, Å	7.795(3)
b, Å	7.889(2)
c, Å	5.5549(11)
V, Å^3	341.6(3)
Z	4
D_{calcd}, g cm^{-3}	3.151
μ, cm^{-1}	10.6
diffractometer/scan	Enraf−Nonius CAD4/ω−2θ
radiation	MoKα (λ = 0.71073 Å)
cryst dimens, mm	0.28 × 0.22 × 0.17
color/shape	slightly yellow fragment
scan widths	0.70 + 0.35 tan θ
min rel transn, %	83.7
decay of standards	<2%
no. of reflections	2722
2θ range, deg	2 < 2θ < 120
range of h, k, l	0−18, 0−19, 0−13
obsd reflcns [I>1σ(I)]	2371
no. of params refined	46
wts	$4F_o^2[\sigma^2(I)+(0.02F_o^2)^2]^{-1}$
$R = \sum\|\Delta F\|/\sum\|F_o\|$	0.045
$R_w = (\sum w(\Delta F)^2/\sum wF^2)^{1/2}$	0.045
GOF	1.677
max. resid density, e Å^{-3}	1.12
min. resid density, e Å^{-3}	−2.01

(III) ion, and is 61 ppm for the 5-coordinate site. The most shielded direction is parallel to the *c*-axis, and also parallel to eq_{zz}. For comparison, for aluminum dissolved in octahedral sites in rutile, the chemical shift anisotropy is estimated at 35 ppm.[94]

TABLE 4: Coordinates and Equivalent Isotropic Displacement Parameters, Andalusite at 115 K

atom	x	y	z	B_{eq} (Å^2)[a]
Al(1)	0	0	0.24177(7)	0.200(4)
Al(2)	0.37014(5)	0.13888(5)	1/2	0.166(4)
Si	0.24590(4)	0.25175(4)	0	0.155(3)
O(1)	0.4229(1)	0.3628(1)	1/2	0.235(7)
O(2)	0.4246(1)	0.3625(1)	0	0.237(7)
O(3)	0.1028(1)	0.4002(1)	0	0.275(8)
O(4)	0.22980(7)	0.13340(7)	0.2395(1)	0.250(5)

[a] $B_{eq} = 8\pi^2/3\sum_i\sum_j U_{ij}\, a_i^*\, a_j^*\, \boldsymbol{a_i a_j}$.

TABLE 5: Bond Distances for Andalusite at 115 K

atoms	distance (Å)	atoms	distance (Å)
Al(1)−O(1)	1.8266(6)	Al(2)−O(3)	1.8393(9)
Al(1)−O(2)	1.8923(6)	Al(2)−O(4)	1.8147(6)
Al(1)−O(4)	2.0776(5)	Si−O(2)	1.6438(9)
Al(2)−O(1)	1.8136(9)	Si−O(3)	1.6173(9)
Al(2)−O(3)	1.8949(9)	Si−O(4)	1.6300(6)

The results of full-crystal DFT calculations are given in Tables 1 and 6. The highest level calculations proved very useful for assigning the NMR spectra and yielded EFG tensors that differ from experiment by less than 1.153 MHz for the *a*,*a* component of the 6-coordinate site and 0.326 MHz for the *a*,*a* component of the 5-coordinate site. Consequently, C_q, η, and the EFG orientation are in excellent agreement with experiment at both Al sites. For example, the orientations of the EFG tensors are calculated to within 0.17° (6-coordinate) and 1.56° (5-coordinate). Figure 3 also shows that the calculated EFG tensor orientation is nearly superimposable with experiment. Andalusite is a favorable case for full-crystal DFT; the unit cell is mid-size, and the lattice structure is rigid, i.e., there is a complete absence of rotating water molecules or highly mobile cations. Application of this method to obtain EFG information has been successful in small crystals, LiN_3, the quadrupole moment of ^{56}Fe, and in systems as large as Mg_2SiO_4, the mineral forsterite.[54,57,58]

The embedded cluster MO results are given in Tables 1 and 6. While C_q and η are in good agreement with experiment, the EFG orientation is less accurate. For instance, the EFG orientation for the 5-coordinate site differs from experiment by about 45° for the angle between eq_{yy} and the *b*-axis of the crystal. The best results are obtained with polarization and without diffuse functions. Adding polarization functions to 6-31G generally increases C_q at the 6-coordinate site and, at the

TABLE 6: Calculated Quadrupole Coupling Constants with Embedded Cluster Molecular Orbital and Full Crystal Density Functional Calculations

	6-coordinate, Al(1) site				5-coordinate, Al(2) site				C_q[Al(1)]:
	C_q/MHz	η	$\angle q_{zz}$ a/°	$\angle q_{yy}$, c/°	C_q/MHz	η	$\angle q_{zz}$ c/°	$\angle q_{yy}$, b/°	C_q[Al(2)]
				experimental values					
	15.261(7)	0.1029(3)	28.50	0	5.8323(8)	0.6733(2)	0	15.87	2.62
				Embedded Cluster Molecular Orbital Theory					
basis set									
6-31G	12.192	0.453	24.77	6.70	−5.650	0.493	75.77	89.34	−2.16
6-31G(d)	12.674	0.340	25.24	4.43	−7.287	0.365	74.80	75.18	−1.74
6-31G(2d)	12.427	0.366	24.85	6.08	−5.065	0.715	73.62	85.46	−2.45
6-31G(3d)	13.549	0.234	27.02	4.47	−4.496	0.966	72.31	88.74	−3.01
6-31G(3df)	15.969	0.139	27.73	59.47	+5.338	0.584	18.50	59.51	+2.99
6-31+G	10.963	0.661	23.32	12.86	−4.021	0.422	61.41	56.13	−2.73
6-31+G(d)	11.290	0.541	23.90	7.83	−5.191	0.470	56.60	36.58	−2.18
6-31+G(2d)	11.646	0.475	23.54	8.35	−5.204	0.337	67.71	61.26	−2.24
6-31+G(3d)	8.641	0.526	13.69	63.99	+4.389	0.775	21.04	70.18	+1.97
6-31+G(3df)	6.775	0.260	18.32	47.10	+5.035	0.547	22.91	46.28	+1.35
cc-pVDZ	12.344	0.404	24.74	4.15	−7.924	0.419	78.67	86.53	−1.56
cc-pVTZ	15.471	0.296	25.56	20.29	4.025	0.858	25.58	74.41	3.84
				Full Crystal Density Functional Theory[a]					
$R_{mt} \times K_{max}$									
3.00	11.638	0.455	31.95	90	1.311	0.706	90	13.17	8.88
3.96	11.546	0.085	28.08	0	5.034	0.883	0	13.48	2.29
4.97	13.933	0.063	28.78	0	5.564	0.717	0	14.19	2.50
5.60	13.491	0.092	28.69	0	5.477	0.783	0	14.68	2.46
6.76	13.639	0.094	28.67	0	5.578	0.764	0	14.31	2.45

[a] V_{xc} = GGA96; G_{max} = 24 a_0^{-1}; k-points = 128.

TABLE 7: Summary of ^{27}Al NMR and NQR of Andalusite

	77 K NQR[6]	previous[3]	this work
6-coordinate site, Al(1)			
C_q/MHz[a]	15.261(3)	15.6	15.261(7)
η	0.106(1)	0.08	0.1029(3)
5-coordinate site, Al(2)			
C_q/MHz	5.960(18)	5.9	5.8323(8)
η	0.700(2)	0.7	0.6733(2)

[a] $C_q = e^2 q_{zz} Q/h$.

5-coordinate site, yields the correct sign only when *f* functions are added. The need for *f* functions is not surprising, since spherical harmonics up to $l = 6$ are needed in the full-crystal DFT calculations. Adding diffuse functions to the 6-31G basis set gives some improvement in the prediction of C_q and η for the 5-coordinate site, but seriously degrades the accuracy for the 6-coordinate site. The same series of polarization and diffuse functions were added to 6-311G, however, the sign remained negative for the 5-coordinate site. A similar change in sign is observed for the 5-coordinate site with the Correlation Consistent Polarized Valence Double (cc-pVDZ) and Triple (cc-pVTZ) Zeta[95,96] basis sets. These differ in contraction scheme and by the addition of an *f* function. On the basis of these considerations, we choose the 6-31G(3df) as the best basis set for andalusite.

The source of the difficulty in calculating accurately C_q, η, and the EFG orientation at the 5-coordinate site becomes apparent upon examination of the two largest eigenvalues of the EFG tensor. These are nearly the same in magnitude but opposite in sign; experimentally, $|q_{yy}/q_{zz}| = 0.84$. For basis sets without sufficient polarization, the eigenvector whose direction most closely parallels the experimental element q_{zz} has the second largest magnitude, rather than the largest magnitude and is thus identified as q_{yy}. Hence, very similar calculated EFG tensors (in the crystal coordinate system) may have the incorrect sign for C_q, depending on the relative values of q_{yy} and q_{zz}. This can be seen in Table 6 by examining the angle between q_{zz} and the *a*-axis. Only with polarization is the ordering of the eigenvalues correct, and even then the orientation of the EFG tensor is not determined well enough to completely interpret the single-crystal NMR results.

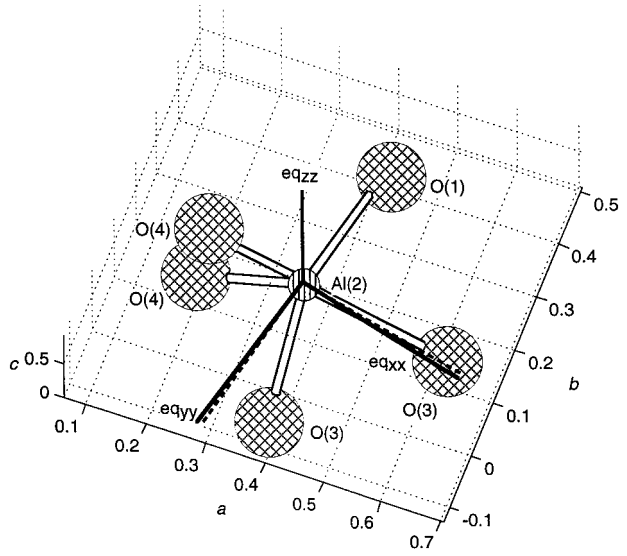

Figure 3. A portion of the andalusite unit cell showing the AlO_5 unit at (x, y, 1/2) and a superimposed axis system for the EFG tensor in its principal axis system, drawn (solid line) in a left-handed coordinate system to better show the correspondence between eq_{xx} and the Al(2)−O(3) bond. The EFG principal axis is parallel to the *c*-axis; one EFG axis must be parallel to *c* as required by the *m* site symmetry at Al(2). The orientation of the EFG tensor calculated with full-crystal DFT methods (dashed line) differs at most by 1.56° from experiment.

The crystal structure of andalusite was determined at 115 K to support 4.2 K NMR experiments. In brief, those experiments indicate no large changes in the EFG tensors for either aluminum site. The linear relationships between cell dimensions and temperature, 25 to 1000 °C, noted by Winter and Ghose,[32] hold for our *b*- and *c*-axes; however, the *a*-axis curve flattens at low temperature, with insignificant change occurring between 25 °C and 115 K. The recent results of Pilati et al.[73] at 25 °C agree

well with those of Winter and Ghose, both for cell dimensions and interatomic distances. The contraction of the axial Al(1)−O(4) distance in the 6-coordinate site with decreasing temperature noted by Winter and Ghose is evident in our 115 K results, with the distance decreasing 2.086(2) Å at 25 °C to 2.0776(5) Å at 115 K. Our data are also consistent with the less steep trends with temperature in the 5-coordinate Al(2) to edge-sharing O distances (Al(2)−O(3)). The Si−O distances are unaffected by temperature.

Conclusions

This work demonstrates that NMR and full-crystal DFT/embedded cluster MO methods can be used to assign EFG tensors to low-symmetry sites, an important first step in developing methods for interpreting ^{27}Al NMR spectra in terms of the aluminum coordination environment. The 6-coordinate site experimental results agree with the previous work of Hafner et al.,[3] and the EFG tensor assignment is the same as found in the point charge analysis of Raymond.[5] The 5-coordinate site is assigned, many years after its first observation, on the basis of full-crystal DFT calculations. This is the first 5-coordinate aluminum site to be fully studied and assigned by NMR. The chemical shift tensor is measured for the 5-coordinate site, and the signs of the quadrupole coupling constants are determined for both the 6- and 5-coordinate sites.

For this moderate size crystal with a well-determined structure, the full-crystal DFT yielded outstanding EFG tensor orientations (within 1.56°) and values of C_q, η sufficiently accurate (to within 11% in the worst case) to aid spectral assignments. Overall, the full-crystal DFT calculations proved superior to embedded cluster MO. Fortunately, the results of the basis set evaluation suggest useful results might be obtained with a larger embedded cluster model. The assessment of calculational accuracy is best made with comparison to results from single-crystal NMR. NMR spectroscopy of ^{27}Al is moving toward multiple field MQMAS experiments on powders and reference calculations, usually with DFT methods. However, we feel it is critically important to assess the accuracy of these calculations with several single-crystal NMR experiments, such as is done in this project.

Acknowledgment. We gratefully acknowledge a grant from the National Science Foundation (CHE-9119871 and CHE-9424021) for the support of this project, and the Louisiana Educational Support Trust Fund for the purchase of the NMR spectrometer and support of C.R.H. Our thanks to Prof. Charles Strouse and Dr. Saeed Khan for the 20 K crystallography work, to Prof. Barbara Dutrow for the loan of the andalusite crystal, and to Prof. Neil Kestner for useful discussions.

Supporting Information Available: One page of anisotropic displacement parameters. This material is available free of charge via the Internet at http://pubs.acs.org.

References and Notes

(1) Kerrick, D. M. *The Al_2SiO_5 Polymorphs*; The Mineralogical Society of America: Washington, DC, 1990; Vol. 22.
(2) Hafner, S.; Raymond, M. *Am. Mineral.* **1967**, *52*, 1632−1641.
(3) Hafner, S. S.; Raymond, M.; Ghose, S. *J. Chem. Phys.* **1970**, *52*, 6037−6041.
(4) Raymond, M.; Hafner, S. S. *J. Chem. Phys.* **1970**, *53*, 4110−4111.
(5) Raymond, M. *Phys. Rev.* **1971**, *B3*, 3692−3702.
(6) Lee, D.; Bray, P. J. *J. Magn. Reson.* **1991**, *94*, 51−58.
(7) Alemany, L. B.; Massiot, D.; Sherriff, B. L.; Smith, M. E.; Taulelle, F. *Chem. Phys. Lett.* **1991**, *177*, 301−306.
(8) Dec, S. F.; Fitzgerald, J. J.; Frye, J. S.; Shatlock, M. P.; Maciel, G. E. *J. Magn. Reson.* **1991**, *93*, 403−406.
(9) Smith, M. E.; Jaeger, C.; Schoenhofer, R.; Steuernagel, S. *Chem. Phys. Lett.* **1994**, *219*, 75−80.
(10) Mundus, C.; Müller-Warmuth, W. *Solid State NMR* **1995**, *5*, 79−88.
(11) Rocha, J. *Chem. Commun.* **1998**, 2489−2490.
(12) Simeral, L. S.; Zens, T.; Finnegan, J. *Appl. Spectrosc.* **1993**, *47*, 1954−1956.
(13) Mason, M. R.; Smith, J. M.; Bott, S. G.; Barron, A. R. *J. Am. Chem. Soc.* **1993**, *115*, 4971−4984.
(14) Nekhaeva, L. A.; Bondarenko, G. N.; Rykov, S. V.; Nekhaev, A. I.; Krentsel, B. A.; Marin, V. P.; Vyshinskaya, L. I.; Khrapova, I. M.; Polonskii, A. V.; Korneev, N. N. *J. Organomet. Chem.* **1991**, *406*, 139−146.
(15) Benn, R.; Rufinska, A.; Janssen, E.; Lehmkuhl, H. *Organometallics* **1986**, *5*, 825−827.
(16) Sugano, T.; Matsubara, K.; Fujita, T.; Takahashi, T. *J. Mol. Catal.* **1993**, *82*, 93−101.
(17) Kimura, Y.; Tanimoto, S.; Yamane, H.; Kitao, T. *Polyhedron* **1990**, *9*, 371−376.
(18) Imhoff, D. W.; Simeral, L. S.; Sangokoya, S. A.; Peel, J. H. *Organometallics* **1998**, *17*, 1941−1945.
(19) Tritto, I.; Donetti, R.; Sacchi, M. C.; Locatelli, P.; Zannoni, G. *Macromolecules* **1997**, *30*, 1247−1254.
(20) Storre, J.; Schnitter, C.; Roesky, H. W.; Schmidt, H.-G.; Nolte-meyer, M.; Fleischer, R.; Stalke, D. *J. Am. Chem. Soc.* **1997**, *119*, 7505−7513.
(21) Wehmschulte, R. J.; Power, P. P. *J. Am. Chem. Soc.* **1997**, *119*, 8387−8388.
(22) Jansen, S. R.; Hintzen, H. T.; Metselaar, R.; Haan, J. W. d.; Ven, L. J. M. v. d.; Kentgens, A. P. M.; Nachtegaal, G. H. *J. Phys. Chem. B* **1998**, *102*, 5969−5976.
(23) Schurko, R. W.; Wasylishen, R. E.; Roerster, H. *J. Phys. Chem. A* **1998**, *102*, 9750−9760.
(24) Ghose, S.; Tsang, T. *Am. Mineral.* **1973**, *58*, 748−755.
(25) Weller, M. T.; Brenchley, M. E.; Apperley, D. C.; Davies, N. A. *Solid State NMR* **1994**, *3*, 103−106.
(26) Engelhardt, G.; Veeman, W. *J. Chem. Soc., Chem. Commun.* **1993**, 622−623.
(27) Janchen, J.; Peeters, M. P. J.; de Haan, J. W.; van de Ven, L. J. M.; van Hooff, J. H. C. *J. Phys. Chem.* **1993**, *97*, 12042−12046.
(28) Peeters, M. P. J.; van de Ven, L. J. M.; de Haan, J. W.; van Hooff, J. H. C. *J. Phys. Chem.* **1993**, *97*, 8254−8260.
(29) Holdaway, M. J.; Mukhopadhyay, B. *Am. Mineral.* **1993**, *78*, 298−315.
(30) Yang, H.; Downs, R. T.; Finger, L. W.; Hazen, R. M.; Prewitt, C. T. *Am. Mineral.* **1997**, *82*, 467−474.
(31) Strouse, C., Khan, S. I., Department of Chemistry, UCLA, unpublished results.
(32) Winter, J. K.; Ghose, S. *Am. Mineral.* **1979**, *64*, 573−586.
(33) Stephenson, D. A.; Moore, P. B. *Acta Crystallogr.* **1968**, *B24*, 1518−1522.
(34) Araki, T.; Finney, J. J.; Zoltai, T. *Am. Mineral.* **1968**, *53*, 1096−1103.
(35) Kato, K.; Saalfeld, H. *Neues Jahrb. Mineral., Abh.* **1968**, *109*, 192−200.
(36) Keegan, T. D.; Araki, T.; Moore, P. B. *Am. Mineral.* **1979**, *64*, 1243−1247.
(37) Higgins, J. B.; Ribbe, P. H.; Nakajima, Y. *Am. Mineral.* **1982**, *67*, 76−84.
(38) Lindop, A. J.; Matthews, C.; Goodwin, D. W. *Acta Crystallogr.* **1975**, *B31*, 2940−2941.
(39) Kutoglu, V. A.; Roesler, A.; Reinen, D. *Z. Anorg. Allg. Chem.* **1979**, *456*, 130−146.
(40) Cruickshank, M. C.; Glasser, L. S. D.; Barri, S. A. I.; Poplett, I. J. F. *J. Chem. Soc., Chem. Commun.* **1986**, 23−24.
(41) Tadanaga, K.; Minami, T.; Tohge, N. *Chem. Lett.* **1994**, 1507−1510.
(42) Hendershot, D. G.; Barber, M.; Kumar, R.; Oliver, J. P. *Organometallics* **1991**, *10*, 3302−3309.
(43) Jegier, J. A.; Atwood, D. A. *Inorg. Chem.* **1997**, *36*, 2034−2039.
(44) Müller, G.; Lachmann, J.; Rufinska, A. *Organometallics* **1992**, *11*, 2970−2972.
(45) Bennett, J. M.; Cohen, J. M.; Artioli, G.; Pluth, J. J.; Smith, J. V. *Inorg. Chem.* **1985**, *24*, 188−193.
(46) Atwood, D. A.; Hill, M. S.; Jegier, J. A.; Rutherford, D. *Organometallics* **1997**, *16*, 2659−2664.
(47) Gainsford, G. J.; Kemmitt, T.; Milestone, N. B. *Inorg. Chem.* **1995**, *34*, 5244−5251.
(48) Warner, H. E.; Wang, Y.; Ward, C.; Gillies, C. W.; Interrante, L. *J. Phys. Chem.* **1994**, *98*, 12215−12222.
(49) Sugano, S.; Shulman, R. G. *Phys. Rev. B.* **1963**, *130*, 517−530.

(50) Mitchell, D. W.; Das, T. P.; Potzel, W.; Schiessl, W.; Harzel, H.; Steiner, M.; Köfferlein, M.; Hiller, U.; Kalvius, G. M.; Martin, A.; Schafer, W.; Will, G.; Halevy, I.; Gal, J. *Phys. Rev. B.* **1996**, *53*, 7684−7698.
(51) Lewandowski, A. C.; Wilson, T. M. *J. Comput. Phys.* **1996**, *129*, 233−242.
(52) Hemmingsen, L.; Ryde, U. *J. Phys. Chem.* **1996**, *100*, 4803−4809.
(53) Palmer, M. H. *Z. Naturforsch. A: Phys. Sci.* **1996**, *51*, 442−450.
(54) Blaha, P.; Schwarz, K.; Herzig, P. *Phys. Rev. Lett.* **1985**, *54*, 1192−1195.
(55) Schwarz, K.; Ambrosch-Draxl, C.; Blaha, P. *Phys. Rev. B* **1990**, *42*, 2051−2061.
(56) Blaha, P.; Singh, D. J.; Sorantin, P. I.; Schwarz, K. *Phys. Rev. B* **1992**, *46*, 1321−1325.
(57) Dufek, P.; Blaha, P.; Schwarz, K. *Phys. Rev. Lett.* **1995**, *75*, 3545−8.
(58) Winkler, B.; Blaha, P.; Schwarz, K. *Am. Mineral.* **1996**, *81*, 545−549.
(59) Karzel, H.; Potzel, W.; Köfferlein, M.; Schiessl, W.; Steiner, M.; Hiller, U.; Kalvius, G. M.; Mitchell, D. W.; Das, T. P.; Blaha, P.; Schwarz, K.; Pasternak, M. P. *Phys. Rev. B* **1996**, *53*, 11425−11438.
(60) Wei, S.-H.; Zunger, A. *J. Chem. Phys.* **1997**, *107*, 1931−1935.
(61) Nagel, S. *J. Phys. C* **1985**, *18*, 3673−3685.
(62) Salasco, L.; Dovesi, R.; Orlando, R.; Causa, M. *Molecular Physics* **1991**, *72*, 267−277.
(63) Sousa, C.; Illas, F.; Pacchioni, G. *J. Chem. Phys.* **1993**, *99*, 6818−6823.
(64) Casanovas, J.; Lorda, A.; Sousa, C.; Illas, F. *Inter. J. Quantum Chem.* **1994**, *52*, 281−293.
(65) Clotet, A.; Ricart, J. M.; Sousa, C.; Illas, F. *J. Electron. Spectrosc. Relat. Phenom.* **1994**, *69*, 65−71.
(66) Brown, A. S.; Spackman, M. A. *J. Phys. Chem.* **1992**, *96*, 9200−9204.
(67) Palmer, M. H.; Blair-Fish, J. A. *Z. Naturforsch* **1994**, *49a*, 137−145.
(68) Vosegaard, T.; Jakobsen, H. J. *J. Magn. Reson.* **1997**, *128*, 135−137.
(69) Huggins, B. A.; Ellis, P. D. *J. Am. Chem. Soc.* **1992**, *114*, 2098−2108.
(70) Tossell, J. A. *Am. Mineral.* **1993**, *78*, 16−22.
(71) Koller, H.; Meijer, E. L.; van Santen, R. A. *Solid State NMR* **1997**, *9*, 165−175.
(72) Schurko, R. W.; Wasylishen, R. E.; Phillips, A. D. *J. Magn. Reson.* **1998**, *133*, 388−394.
(73) Pilati, T.; Demartin, F.; Gramaccioli, C. M. *Acta Crystallogr.* **1997**, *B53*, 82−94.
(74) Eichele, K.; Washylishen, R. E.; Corrigan, J. F.; Taylor, N. J.; Carty, A. J. *J. Am. Chem. Soc.* **1995**, *117*, 6961−6969.
(75) Power, W. P.; Mooibroek, S.; Wasylishen, R. E.; Cameron, T. S. *J. Phys. Chem.* **1994**, *98*, 1552−1560.
(76) Volkoff, G. M.; Petch, H. E.; Smellie, D. W. L. *Can. J. Phys.* **1952**, *30*, 270−289.
(77) Berglund, B.; Tegenfeldt, J. *J. Magn. Reson.* **1978**, *30*, 451−455.
(78) Burnham, C. W.; Buerger, M. J. *Z. Kristallogr.* **1961**, *115*, 269−290.
(79) Fair, C. K. *MolEN, An Interactive Structure Solution Procedure*; Delft: The Netherlands, **1990**.
(80) *Gaussian 92/DFT*, Revision F.4, Frisch, M. J.; Trucks, G. W.; Schlegel, H. B.; Gill, P. M. W.; Johnson, B. G.; Wong, M. W.; Foresman, J. B.; Robb, M. A.; Head-Gordon, M.; Replogle, E. S.; Gomperts, R.; Andres, J. L.; Raghavachari, K.; Binkley, J. S.; Gonzalez, C.; Martin, R. L.; Fox, D. J.; Defrees, D. J.; Baker, J.; Stewart, J. J. P.; Pople, J. A. Gaussian, Inc.: Pittsburgh, PA, 1993.
(81) Halkier, A.; Koch, H.; Christiansen, O.; Jörgensen, P.; Helgaker, T. *J. Chem. Phys.* **1997**, *107*, 849−866.
(82) Mitchell, D. W.; Sulaimam, S. B.; Sahoo, N.; as, T. P.; Potzel, W.; Kalvius, G. M. *Phys. Rev. B* **1991**, *44*, 6728−6730.
(83) Cummins, P. L.; Bacskay, G. B.; Hush, N. S. *J. Chem. Phys.* **1987**, *86*, 6908−6917.
(84) Wilson, S. Basis Sets. In *Ab Initio Methods in Quantum Chemistry−Part 1*; Lawley, K. P., Ed.; John Wiley and Sons Ltd.: New York, 1987.
(85) Dunning, T. H., Jr.; Hay, P. J. Gaussian Basis Sets for Molecular Calculations. In *Methods of Electronic Structure Theory*; Schaefer, H. F., III., Ed.; Plenum Press: New York, 1977; pp 1−27.
(86) *WIEN97.5* Blaha, P.; Schwarz, K.; Luitz, J. WIEN97, Vienna University of Technology 1997. (Improved and updated Unix version of the original copyrighted WIEN code, which was published by Blaha, P.; Schwarz, K.; Sorantin, P.; Trickey, S. B. *Comput. Phys. Commun.* **1990**, *59*, 399−415).
(87) Perdew, J. P.; Burke, K.; Ernzerhof, M. *Phys. Rev. Lett.* **1996**, *77*, 3865−3868.
(88) Perdew, J. P.; Wang, Y. *Phys. Rev.* **1992**, *B45*, 13244−13249.
(89) Singh, D. *Plane waves, pseudopotentials and the LAPW method*; Kluwer Academic Publishers: Boston, 1994.
(90) Pyykkö, P. *Z. Naturforsch* **1992**, *47a*, 189−196.
(91) Conversion factors, $e^2qQ/h = eQ/h \times V/\mathrm{m}^{-2} = 3.3924 \times 10^{-21}$ MHz/(V m^{-2}) (for DFT calculations with eq in V m^{-2}). $e^2qQ/h = e^2Q/(4\pi\epsilon a_o^3 h) \times (-1) \times (q_{zz}) = -32.966$ MHz/au (for *Gaussian92*/DFT calculations that report $-q$ in atomic units).
(92) Gerald, R., II; Bernhard, T.; Haeberlen, U.; Rendell, J.; Opella, S. *J. Am. Chem. Soc.* **1993**, *115*, 777−782.
(93) Haeberlen, U. *High Resolution NMR in Solids: Selective Averaging*; Academic Press: New York, 1976.
(94) Stebbins, J. F.; Famaon, I.; Klabunde, U. *J. Am. Ceram. Soc.* **1989**, *72*, 2198−2200.
(95) Dunning, T. H., Jr. *J. Chem. Phys.* **1989**, *90*, 1007−1023.
(96) Woon, D. E.; Dunning, T. H., Jr. *J. Chem. Phys.* **1993**, *98*, 1358−1371.